LONGITUDINAL POCHHAMMER – CHREE WAVES IN MILD AUXETICS AND NON-AUXETICS

A. V. Ilyashenko

Moscow State University of Civil Engineering
Moscow, Russia

S. V. Kuznetsov*

Institute for Problems in Mechanics
Moscow, Russia

ABSTRACT

The exact solutions of Pochhammer – Chree equation for propagating harmonic waves in isotropic elastic cylindrical rods, are analyzed. Spectral analysis of the matrix dispersion equation for the longitudinal axially symmetric modes is performed. Analytical expressions for displacement fields are obtained. Variation of the wave polarization due to variation of Poisson's ratio for mild auxetics (Poisson's ratio is greater than -0.5) is analyzed and compared with the non-auxetics. It is observed that polarization of the waves for both considered cases (auxetics and non-auxetics) exhibits abnormal behavior in the vicinity of the bulk shear wave speed.

Keywords: Auxetics, Dispersion, Pochhammer – Chree wave, Polarization.

1. INTRODUCTION

The equation for propagating harmonic waves in a cylindrical rod, now known as the Pochhammer – Chree equation, was for the first time derived in [1-3]. However, the corresponding solutions binding the phase or group speed with frequency remained unexplored until mid of the last century, when the first branches of the dispersion curves were obtained numerically in [4-22]. In [4-20] longitudinal axially symmetric modes were explored, and in [21, 22] flexural and torsional modes were also considered. According to [16] the axially symmetric longitudinal modes are denoted by $L(0, m)$, where m is the mode number.

In [4-6] by asymptotic methods applied to dispersion relations were obtained analytical formulas for both short-wave ($c_{1,\lim}$) and long-wave ($c_{2,\lim}$) limits. Following [6] (see also [15]), the short-wave limit speed ($c_{1,\lim}$) at $\omega \to \infty$

$$c_{1,\lim} = c_R \tag{1}$$

coincides with Rayleigh wave speed (c_R), while the long-wave limit speed $c_{2,\lim}$ yields [15]

$$c_{2,\lim} = \sqrt{\frac{E}{\rho}}, \tag{2}$$

where E is Young's modulus, and ρ is the material density. In [6, 15] the long-wave limit $c_{2,\lim}$ was named as the "rod" wave speed.

Dispersion curves related to higher axially symmetric modes were studied in [4-20]. In [8] the first several roots of the dispersion equation were (numerically) obtained and it was revealed that some of the roots were complex relating to attenuating modes. Beside dispersion curves, variation of the displacement magnitudes along radius of the rod for the first three $L(0, m)$ modes at fixed Poisson's ratio $\nu = 0.3317$ was analyzed in [19].

One of the interesting peculiarities of propagating $L(0, m)$, $m > 1$ modes at $\gamma \to 0$, where γ is the wave number ($\gamma = 2\pi/l$, l is the wavelength), corresponds to the zero slope of the dimensionless frequency Ω [15]:

$$\lim_{\gamma \to 0} \frac{\partial \Omega}{\partial \gamma} = 0. \tag{3}$$

In (3) $\Omega = \omega R/c_2$ is the dimensionless frequency; ω is the circular frequency, R is a radius of the rod; c_2 is the velocity of the bulk shear wave. Actually, condition (3) means presence of the horizontal asymptote in the dispersion relation $\omega(c)$ at $c \to \infty$. Resemblance with the dispersion curves at $c \to \infty$ for higher modes of Lamb and Love waves can be observed, see [23, 24].

Extensions of the Pochhammer – Chree waves to hel-

* Corresponding author (kuzn-sergey@yandex.ru)

DOI : 10.1017/jmech.2018.13
Copyright © 2018 The Society of Theoretical and Applied Mechanics
https://doi.org/10.1017/jmech.2018.13 Published online by Cambridge University Press

ical waves (longitudinal axially symmetric modes) that relate to non-integer coefficients at the angle coordinate in the corresponding potentials, were analyzed in [25-27].

The current research is devoted to the spectral analysis of the matrix dispersion equation for the longitudinal axially symmetric Pochhammer – Chree waves. Analytical expressions for the displacement fields are obtained, presumably, for the first time. Variation of the wave polarization due to variation of Poisson's ratio for mild auxetics (Poisson's ratio is greater than -0.5) was analyzed and compared with the non-auxetics. It was also observed that polarization of the waves for both cases (auxetics and non-auxetics) exhibits abnormal behavior in the vicinity of the bulk shear wave speed. The latter phenomenon can have various applications, e.g. design of the acoustical filters preventing propagation of the considered Pochhammer – Chree waves at frequencies corresponding to the bulk shear wave speed.

2. GOVERNING EQUATIONS

Equation of motion for an isotropic medium at absence of body forces can be written in the form

$$c_1^2\nabla\mathrm{div}\,\mathbf{u}-c_2^2\mathrm{rot}\,\mathrm{rot}\,\mathbf{u}=\partial_{tt}^2\mathbf{u}, \tag{4}$$

where $\mathbf{u}$ is the displacement field, c_1, c_2 are speeds of bulk longitudinal and shear waves respectively, and

$$c_1=\sqrt{\frac{\lambda+2\mu}{\rho}},\quad c_2=\sqrt{\frac{\mu}{\rho}}. \tag{5}$$

In (5) λ, μ are Lame's constants, and ρ is the material density.

The Helmholtz representation for the displacement field $\mathbf{u}$ yields

$$\mathbf{u}=\nabla\Phi+\mathrm{rot}\boldsymbol{\Psi}, \tag{6}$$

where Φ and $\boldsymbol{\Psi}$ are scalar and vector potentials respectively. In cylindrical coordinates representation (6) for the physical components of the displacement field, becomes (see definition for physical components in [28])

$$\begin{aligned}
u_r&=\frac{\partial\Phi}{\partial r}+\frac{1}{r}\frac{\partial\Psi_z}{\partial\theta}-\frac{\partial\Psi_\theta}{\partial z}\\
u_\theta&=\frac{1}{r}\frac{\partial\Phi}{\partial\theta}+\frac{\partial\Psi_r}{\partial z}-\frac{\partial\Psi_z}{\partial r}\\
u_z&=\frac{\partial\Phi}{\partial z}+\frac{1}{r}\frac{\partial}{\partial r}\left(r\Psi_\theta\right)-\frac{1}{r}\frac{\partial\Psi_r}{\partial\theta},
\end{aligned} \tag{7}$$

In (7) it is assumed that coordinate z directs along the central axis of the rod; r is the radial coordinate; θ is the circumferential coordinate; and Ψ_r, Ψ_θ, Ψ_z are components of the vector potential $\boldsymbol{\Psi}$ in the cylindrical coordinates.

Substituting (6) into equation of motion (4) yields

$$c_1^2\Delta\Phi=\ddot{\Phi},\quad c_2^2\Delta\boldsymbol{\Psi}=\ddot{\boldsymbol{\Psi}}. \tag{8}$$

For a harmonic wave propagating along axis z, potentials (8) can be represented in a form

$$\Phi=\Phi_0(\boldsymbol{x}')e^{i\gamma(z-ct)},\quad \boldsymbol{\Psi}=\boldsymbol{\Psi}_0(\boldsymbol{x}')e^{i\gamma(z-ct)}, \tag{9}$$

where, as before, γ is the wave number related to the phase speed c and circular frequency ω by equation

$$\gamma=\frac{\omega}{c}. \tag{10}$$

In (9) $\boldsymbol{x}'$ is the (vector) coordinate in the cross section of a rod ($\mathbf{x}'=\mathbf{x}-(\mathbf{n}\cdot\mathbf{x})\mathbf{n}$), $\mathbf{n}$ is the wave vector; and $z=\mathbf{n}\cdot\mathbf{x}$.

Substituting representations (9) into Eq. (8), yields the Helmholtz equations for the potentials

$$\Delta\Phi_0+\left(\frac{c^2}{c_1^2}-1\right)\gamma^2\Phi_0=0,\quad \Delta\boldsymbol{\Psi}_0+\left(\frac{c^2}{c_2^2}-1\right)\gamma^2\boldsymbol{\Psi}_0=0. \tag{11}$$

Axial symmetry of Φ_0 ensures [13, 14]

$$\frac{\partial\Phi_0}{\partial\theta}=0. \tag{12}$$

Equations (11), (12) result in Bessel's equation

$$\frac{1}{r}\frac{d}{dr}r\frac{d}{dr}\Phi_0(r)+\left(\frac{c^2}{c_1^2}-1\right)\gamma^2\Phi_0(r)=0, \tag{13}$$

where c is the phase speed. The solution of Eq. (13) can be represented in terms of the corresponding Bessel functions

$$\Phi_0(r)=C_1J_0(q_1r)+C_3Y_0(q_1r), \tag{14}$$

where C_k, k = 1,3 are the unknown complex coefficients, and

$$q_1^2=\left(\frac{c^2}{c_1^2}-1\right)\gamma^2. \tag{15}$$

Axial symmetry of potential $\boldsymbol{\Psi}_0$ is satisfied by the following Eqs. [13, 14]

$$\frac{\partial\Psi_r}{\partial\theta}=\frac{\partial\Psi_\theta}{\partial\theta}=\frac{\partial\Psi_z}{\partial\theta}=0. \tag{16}$$

Equations (11), (16) yield Bessel equations (for physical components)

$$\begin{aligned}
&\frac{1}{r}\frac{d}{dr}r\frac{d}{dr}\Psi_r(r)+\left(\left(\frac{c^2}{c_2^2}-1\right)\gamma^2-\frac{1}{r^2}\right)\Psi_r(r)=0\\
&\frac{1}{r}\frac{d}{dr}r\frac{d}{dr}\Psi_\theta(r)+\left(\left(\frac{c^2}{c_2^2}-1\right)\gamma^2-\frac{1}{r^2}\right)\Psi_\theta(r)=0\\
&\frac{1}{r}\frac{d}{dr}r\frac{d}{dr}\Psi_z(r)+\left(\frac{c^2}{c_2^2}-1\right)\gamma^2\Psi_z(r)=0.
\end{aligned} \tag{17}$$

The solutions of Eq. (17) are

https://doi.org/10.1017/jmech.2018.13 Published online by Cambridge University Press

$$\Psi_\theta(r) = C_2 J_1(q_2 r) + C_4 Y_1(q_2 r)$$
$$\Psi_r(r) = C_5 J_1(q_2 r) + C_6 Y_1(q_2 r)$$
$$\Psi_z(r) = C_7 J_0(q_2 r) + C_8 Y_0(q_2 r). \quad (18)$$

In (18) C_k, k = 2, 4, …, 8 are the unknown complex coefficients, and

$$q_2^2 = \left(\frac{c^2}{c_2^2} - 1\right)\gamma^2. \quad (19)$$

Axial symmetry of the vector potential $\mathbf{\Psi}$ imposes another restriction [14, 16]:

$$\Psi_r = \Psi_z = 0. \quad (20)$$

Now, accounting (7), (14), (18), (20), the desired vector field corresponding to the propagating longitudinal axially symmetric harmonic wave, becomes [19]

$$u_r = -\begin{bmatrix} q_1\left(C_1 J_1(q_1 r) + C_3 Y_1(q_1 r)\right) \\ +i\gamma\left(C_2 J_1(q_2 r) + C_4 Y_1(q_2 r)\right)\end{bmatrix} e^{i\gamma(z-ct)}$$
$$u_\theta = 0$$
$$u_z = \begin{bmatrix} i\gamma\left(C_1 J_0(q_1 r) + C_3 Y_0(q_1 r)\right) \\ +q_2\left(C_2 J_0(q_2 r) + C_4 Y_0(q_2 r)\right)\end{bmatrix} e^{i\gamma(z-ct)}. \quad (21)$$

Since components (21) vector field should be finite at r = 0 and noting that at $r \to 0$ Bessel's functions Y_0, Y_1 are unbounded, the final representation flows out from (21)

$$u_r = -\left[q_1 C_1 J_1(q_1 r) + i\gamma C_2 J_1(q_2 r)\right] e^{i\gamma(z-ct)}$$
$$u_z = \left[i\gamma C_1 J_0(q_1 r) + q_2 C_2 J_0(q_2 r)\right] e^{i\gamma(z-ct)}, \quad u_\theta = 0. \quad (22)$$

Remark 2.1 Expressions (22) that at r = 0 the natural condition u_r = 0 is satisfied since $J_1(0)$ = 0. At the same time $J_1(0)$ = 0, so u_z at r = 0 takes the form

$$u_z = \left[i\gamma C_1 + q_2 C_2\right] e^{i\gamma(z-ct)}. \quad (23)$$

Expression (23) gives the following necessary and sufficient condition for vanishing u_z at r = 0

$$i\gamma C_1 = -q_2 C_2. \quad (24)$$

Condition (24) ensures the non-disturbance of the rod axis at propagating Pochhammer – Chree wave.

3. DISPERSION EQUATION

Traction free boundary conditions on a lateral cylindrical surface at $r = R$ have the form

$$\mathbf{t}_\nu \equiv \left(\lambda(\mathrm{tr}\boldsymbol{\varepsilon})\boldsymbol{\nu} + 2\mu\boldsymbol{\varepsilon}\cdot\boldsymbol{\nu}\right)\Big|_{r=R} = 0, \quad (25)$$

where $\boldsymbol{\nu}$ is the (outward) surface normal; λ, μ are Lame's constants.

Substituting the displacements (22) into boundary conditions (25), yields the following equations

$$t_{rr} \equiv \lambda I_\varepsilon + 2\mu\varepsilon_{rr}$$
$$= -\begin{bmatrix} \lambda\left(q_1^2 + \gamma^2\right) J_0(q_1 r) C_1 \\ +\dfrac{2\mu}{r}\begin{bmatrix} q_1 C_1\left(q_1 r J_0(q_1 r) - J_1(q_1 r)\right) \\ +i\gamma C_2\left(q_2 r J_0(q_2 r) - J_1(q_2 r)\right)\end{bmatrix}\end{bmatrix}_{r=R} = 0$$
$$t_{rz} \equiv 2\mu\varepsilon_{rz}$$
$$= -\mu\begin{bmatrix} i\gamma\left[q_1 C_1 J_1(q_1 r) + i\gamma C_2 J_1(q_2 r)\right] \\ +\left[i\gamma q_1 C_1 J_1(q_1 r) + q_2^2 C_2 J_1(q_2 r)\right]\end{bmatrix}_{r=R} = 0. \quad (26)$$

where the exponential multiplier $e^{i\gamma(z-ct)}$ is omitted. Equation (26) can be given in the matrix form as follows:

$$\det \mathbf{A} = 0, \quad (27)$$

where $\mathbf{A}$ is a square and generally non-symmetric 2 × 2 matrix with complex coefficients

$$A_{11} = -\left(\left(q_1^2 + \gamma^2\right)\frac{c_1^2}{c_2^2} - 2\gamma^2\right) J_0(q_1 R) + \frac{2q_1}{R} J_1(q_1 R)$$
$$A_{12} = -\frac{2i\gamma}{R}\left(q_2 R J_0(q_2 R) - J_1(q_2 R)\right)$$
$$A_{21} = -2i\gamma q_1 J_1(q_1 R)$$
$$A_{22} = -\left(q_2^2 - \gamma^2\right) J_1(q_2 R). \quad (28)$$

$\vec{C}$ is the vector of unknown coefficients and $\vec{\mathbf{0}}$ is the zero-vector. Note that for getting Eq. (27) from Eq. (26) the identity

$$\frac{\lambda}{\mu} = \frac{c_1^2}{c_2^2} - 2. \quad (29)$$

was used. The existence of non-trivial solutions to Eq. (27) implies the dispersion equation

$$\mathbf{A}\cdot\vec{C} = 0, \quad (30)$$

Two-dimensional (right) eigenvectors related to vanishing eigenvalues (kernel eigenvalues) of matrix $\mathbf{A}$ define polarization of the corresponding Pochhammer – Chree waves.

Dispersion Eq. (27) can have both real and imaginary and complex roots [13-15]. Real roots correspond to propagating modes without attenuation in z direction, while imaginary and complex roots correspond to non-propagating modes attenuating in z direction. Herein, only propagating modes will be analyzed.

Substituting components (28) into Eq. (27) yields the dispersion equation in the form [19]

https://doi.org/10.1017/jmech.2018.13 Published online by Cambridge University Press

$$4\gamma^2 q_1 q_2 J_0(q_2 R) J_1(q_1 R) - \frac{2q_1}{R}\left(q_2^2+\gamma^2\right) J_1(q_1 R) J_1(q_2 R)$$
$$+\left(q_2^2-\gamma^2\right)\left((q_1^2+\gamma^2)\frac{c_1^2}{c_2^2}-2\gamma^2\right) J_0(q_1 R) J_1(q_2 R) = 0. \tag{31}$$

4. SPECTRAL ANALYSIS OF MATRIX A

Spectral analysis of matrix **A** splits into two cases.

4.1 Matrix A is (Semi) Simple

That is the case when matrix **A** contains no Jordan blocks, and hence has two distinct eigenvectors. Spectral decomposition of **A** yields

$$\vec{\alpha}_1 \leftrightarrow \lambda_1, \quad \vec{\alpha}_2 \leftrightarrow \lambda_2 \tag{32}$$

where λ_1, λ_2 are right eigenvalues of matrix **A**, and $\vec{\alpha}_1, \vec{\alpha}_2$ are two-dimensional eigenvectors. The characteristic equation for matrix **A** written in the form

$$\det\left(\mathbf{A}-\lambda\mathbf{I}\right)=0, \tag{33}$$

where **I** is the unit diagonal matrix, yields the following representations for eigenvalues

$$\lambda_{1,2} = s \pm d, \tag{34}$$

in (33)

$$s=\frac{A_{11}+A_{22}}{2}, \quad d=\sqrt{f^2+A_{12}A_{21}}, \quad f=\frac{A_{11}-A_{22}}{2} \tag{35}$$

Note, that coefficients A_{ij} in (35) are defined by (28).

The corresponding (normed) eigenvectors have the form

$$\vec{\alpha}_{1,2}=\begin{pmatrix} \dfrac{f\pm d}{\sqrt{|A_{21}|^2+|f\pm d|^2}} \\ \dfrac{A_{21}}{\sqrt{|A_{21}|^2+|f\pm d|^2}} \end{pmatrix}. \tag{36}$$

Analyses of expressions (34) and (36) allow formulating

Proposition 4.1

a) The necessary and sufficient condition for simplicity of matrix **A** is

$$d \neq 0, \tag{37}$$

where discriminant d is defined by (35).

b) Condition for degeneracy of matrix **A** takes the form

$$A_{11}A_{22} = A_{12}A_{21}. \tag{38}$$

Proof.

a) Expression (34) reveals, that condition (37) gives a necessary and sufficient condition for simplicity of the considered matrix.

b) Due to (34), condition of degeneracy takes the form

$$s^2 = d^2. \tag{39}$$

Equation (39) with account of (35) yields the desired Eq. (38).

Remark 4.1 The straightforward analysis reveals that condition (38) is equivalent to the dispersion Eq. (27).

4.2 Matrix A is Non-Semisimple (Contains Jordan Block)

Condition for non-simplicity of matrix **A** following from expression (34), yields

$$d = 0. \tag{40}$$

At (40) the spectral decomposition of matrix **A** results

$$\begin{pmatrix} \dfrac{f}{\sqrt{|A_{21}|^2+|f|^2}} \\ \dfrac{A_{21}}{\sqrt{|A_{21}|^2+|f|^2}} \end{pmatrix} \leftrightarrow \lambda_{1,2} = s. \tag{41}$$

Thus, at (40) matrix **A** becomes not only non-simple matrix, but non-semisimple as well, since it has only one (right) eigenvector (41).

At (40) and in view of (34) the double degeneracy of **A** is equivalent to

$$s = 0. \tag{42}$$

Now, taking into account (35), the following proposition flows out

Proposition 4.2

a) The necessary and sufficient condition for non-semisimplicity of matrix **A** is

$$f^2 = -A_{12}A_{21}. \tag{43}$$

b) At condition (43) double degeneracy of matrix **A** takes the form

$$A_{11} = -A_{22}. \tag{44}$$

Proof.

a) Proposition 4.1.a ensures that at (40) matrix **A** becomes non-simple. But, at (40) both eigenvectors coincide due to (36), so, actually **A** becomes non-semisimple. Then, substituting expressions (35) into (40) yields condition (43).

b) Due to (34), degeneracy of matrix **A** at (40) is equivalent to

$$s = 0. \tag{45}$$

But, (45) is equivalent to (44).

Remark 4.2 For the considered case of degeneracy

https://doi.org/10.1017/jmech.2018.13 Published online by Cambridge University Press

of the non-semisimple matrix, the corresponding dispersion equation takes the form

$$\left(q_2^2-\gamma^2\right)^2\left(J_1(q_2R)\right)^2-\gamma^2q_1q_2J_0(q_2R)J_1(q_1R)$$
$$+\frac{\gamma^2q_1}{R}J_1(q_2R)J_1(q_1R)=0. \qquad (46)$$

5. DISPLACEMENT FIELDS

Components of the kernel eigenvectors (36), (41), that correspond to vanishing eigenvalues, are coefficients C_1, C_2 in expressions (22). Depending on the spectral properties of matrix **A**, two cases are considered.

5.1 Displacements at (Semi) Simple Matrix

Substituting components of the kernel eigenvector (36) that corresponds to vanishing eigenvalue (34) into (22) at condition (38), yields

$$u_r=\frac{-\left[q_1\left(f\pm d\right)J_1(q_1r)+i\gamma A_{21}J_1(q_2r)\right]}{\sqrt{\left|A_{21}\right|^2+\left|f\pm d\right|^2}}e^{i\gamma(z-ct)}$$
$$u_z=\frac{\left[i\gamma\left(f\pm d\right)J_0(q_1r)+q_2A_{21}J_0(q_2r)\right]}{\sqrt{\left|A_{21}\right|^2+\left|f\pm d\right|^2}}e^{i\gamma(z-ct)}, \qquad (47)$$

where f, d are defined by (35), and coefficients A_{ij} of matrix **A** are defined by (28). In (47) and further vanishing component u_θ is not present.

Proposition 5.1 For (semi) simple matrix **A** the displacement component u_z vanishes at $r = 0$ and at $c = c_2$ regardless of frequency and Poisson's ratio.

Proof. For the considered case condition (24) takes the form

$$i\gamma\left(f\pm d\right)=-q_2A_{21}. \qquad (48)$$

Equation (48) with account of (35) can be transformed to the equivalent equation:

$$i\gamma q_2\left(A_{11}-A_{22}\right)+q_2^2A_{21}+\gamma^2A_{12}=0. \qquad (49)$$

Substituting expressions (28) into (49) at $c = c_2$ ensures vanishing u_z at $r = 0$.

Corollary. For the considered simple matrix **A**, expressions (47) are applicable for any axially symmetric mode $L(0, m)$, $m > 0$.

Remark 5.1 For very low negative Poisson's ratio values ($\nu < -0.5$) the phase speed c_2 exceeds $c_{2,\mathrm{lim}}$; see expressions (2) and (5) with account of expression for Lame's constant

$$\mu=\frac{E}{2(1+\nu)} \qquad (50)$$

Thus, for $-1 < \nu < -0.5$ vanishing speed c_2 does not belong to the interval ($c_{1,\mathrm{lim}}$; $c_{2,\mathrm{lim}}$) where the longitudinal fundamental mode exists. However, higher modes of longitudinal Pochhammer – Chree waves exist at c_2 and, as the Proposition 4.1 ensures, the corresponding displacement fields vanish at this speed.

5.2 Displacements at Non-Semisimple Matrix

Substituting components of the kernel eigenvector (41) into (22) with account of conditions of degeneracy (43), (44), yield

$$u_r=\frac{-\left[q_1f\,J_1(q_1r)+i\gamma A_{21}J_1(q_2r)\right]}{\sqrt{\left|A_{21}\right|^2+\left|f\right|^2}}e^{i\gamma(z-ct)}$$
$$u_z=\frac{\left[i\gamma\,f\,J_0(q_1r)+q_2A_{21}J_0(q_2r)\right]}{\sqrt{\left|A_{21}\right|^2+\left|f\right|^2}}e^{i\gamma(z-ct)}. \qquad (51)$$

Proposition 5.2 For a non-semisimple matrix **A** the displacement component u_z does not vanish at $r = 0$ and at $c = c_2$ regardless of frequency.

Proof. For the considered case condition (24) takes the form

$$i\gamma\,f=-q_2A_{21}. \qquad (52)$$

Equation (52) with account of (35) can be transformed to the equivalent equation

$$i\gamma\left(A_{11}-A_{22}\right)+2q_2A_{21}=0. \qquad (53)$$

Substituting (28) into (53) at $c = c_2$ reveals that condition (52) does not hold.

Corollary. For the considered non-semisimple matrix **A**, expressions (47) are applicable for any axially symmetric mode $L(0, m)$, $m > 0$.

5.3 Displacements on Lateral Surface

Normalized amplitudes U_r, U_z of the displacement fields on a cylinder lateral surface at $r = R$ can be defined by the following formulas

$$U_r\equiv\left.\frac{\left|u_r\right|}{\left|u_r\right|+\left|u_z\right|+1}\right|_{r=R}$$
$$U_z\equiv\left.\frac{\left|u_z\right|}{\left|u_r\right|+\left|u_z\right|+1}\right|_{r=R}. \qquad (54)$$

Remark 5.3 Generally, amplitude values of the components $|u_r|$ and $|u_z|$ can simultaneously vanish at some value of the radius, and particularly they can vanish at $r = R$. For this reason unity is added to the denominators in (54).

https://doi.org/10.1017/jmech.2018.13 Published online by Cambridge University Press

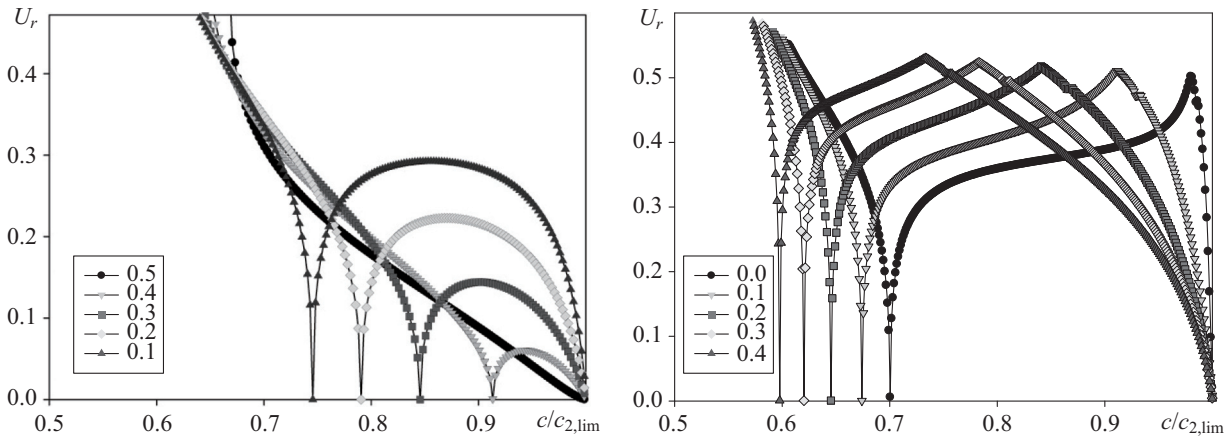


Fig. 1 Displacement component U_r variation vs phase velocity.

6. ABNORMALITY OF THE WAVE FIELD AT C_2 PHASE SPEED

Substituting phase speed $c = c_2$ into (28) reveals that at c_2 matrix **A** is semi simple with the following one kernel (right) eigenvector

$$\begin{pmatrix} 0 \\ 1 \end{pmatrix} \leftrightarrow \lambda = 0. \tag{55}$$

Eigenvector (55) corresponds to the following coefficients in representation (22):

$$C_1 = 0, \quad C_2 = 1. \tag{56}$$

Analysis of expressions (28) and (47) for the considered case reveals that at $c = c_2$ both displacement components u_r and u_z vanish regardless of the circular frequency. Indeed, in view of (47), (48) at $c \to c_2 \pm 0$ the displacement components become

$$u_r = \frac{A_{21}\left[-\dfrac{q_1 q_2}{i\gamma} J_1(q_1 r) + i\gamma J_1(q_2 r)\right]}{\sqrt{\left|A_{21}\right|^2 + \left|f \pm d\right|^2}} e^{i\gamma(z-ct)}$$

$$u_z = \frac{q_2 A_{21}\left[-J_0(q_1 r) + J_0(q_2 r)\right]}{\sqrt{\left|A_{21}\right|^2 + \left|f \pm d\right|^2}} e^{i\gamma(z-ct)}, \tag{57}$$

with (non zero) A_{21} being defined by (28). Taking into account that $q_2 = 0$ at $c = c_2$ allows us to formulate

Proposition 6.1. No Pochhammer – Chree $L(0, m)$, $m > 0$ waves can propagate at the phase speed coinciding with c_2 speed.

In the following section numerical study of the displacement amplitudes U_r and U_z variation with the phase speed, will reveal that these components simultaneously vanish in the vicinity of c_2 speed, independently of Poisson's ratio variation in the interval $\nu \in [-0.4, 0.4]$.

7. DISPLACEMENT FIELDS OF THE FUNDAMENTAL MODE

Displacement components are defined by expressions (47) for a simple matrix (it can be shown that for the fundamental mode the non-semisimplicity cannot arise). Amplitudes U_r, U_z on a free surface of the cylinder are defined by Eq. (54). The amplitudes U_r, U_z will be analyzed at different values of Poisson's ratio varied in the interval $\nu \in [-0.5, 0.4]$.

7.1 Amplitude U_r

Variation of the displacement amplitude U_r related to the fundamental mode with respect to variation of the phase speed, is plotted in Fig. 1. The presented plots correspond to different values of Poisson's ratio indicated in the legend (left plot relates to negative, while right one to positive values of Poisson's ratio).

The most interesting in Fig. 1 is vanishing of the amplitude U_r at the phase speed $c \to c_2 \pm 0$ and at $c \to c_{2,\lim} - 0$.

7.2. Amplitude U_z

Variation of the displacement amplitude U_z related to the fundamental mode with respect to variation of the phase speed, is plotted in Fig. 2. Again, the plots correspond to different values of Poisson's ratio indicated in the legend, and left plot relates to negative, while right one to positive values of Poisson's ratio.

Herein, for positive values of Poisson's ratio the displacement amplitude U_z (Fig. 2(b)) vanishes at two values of the phase speed related to c_2 and another speed c_k. The latter speed depends upon Poisson's ratio and can be approximated by the following fraction-rational expression

$$c_k \approx \frac{c_{2,\lim}}{a + b\nu}, \quad a = 1.0126, \quad b = 0.8889 \tag{58}$$

https://doi.org/10.1017/jmech.2018.13 Published online by Cambridge University Press

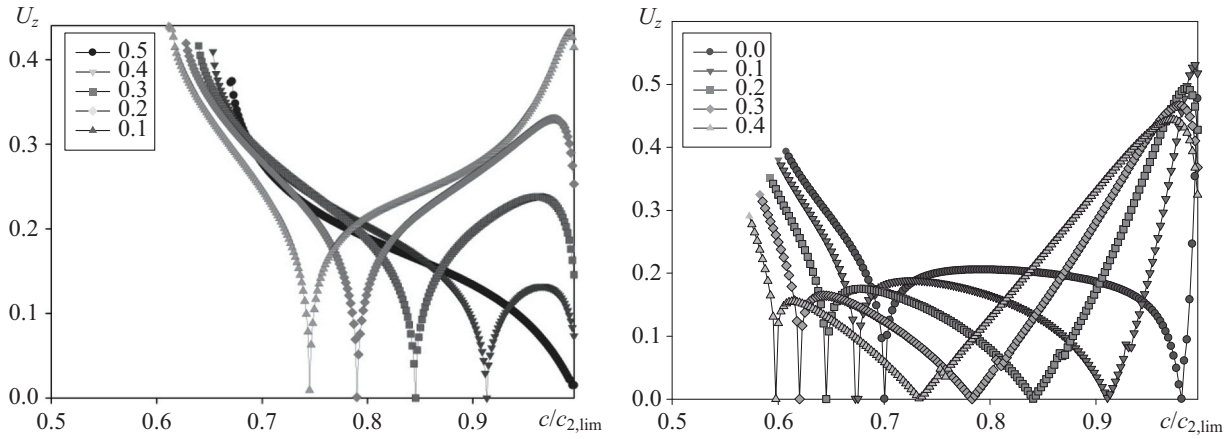


Fig. 2 Displacement component U_z variation vs phase velocity.

At higher speeds than c_k the component U_z gradually rises to about 0.5. Parameters a, b in (58) are found by the regression analysis. The obtained values for a, b in (58) ensure relative error not exceeding 0.1% for the considered Poisson's ratio values $\nu \in (0, 0.4)$. At negative Poisson's ratios (Fig. 2(a)) the displacement amplitude U_z vanishes at $c \to c_2 \pm 0$ only.

Observance (at positive Poisson's ratio values) of the phase speed c_k, at which $U_z = 0$, but $U_r \neq 0$, may have various applications in NDT, e.g. determining Poisson's ratio by measuring speed c_k and inverting expression (58):

$$\nu = \frac{1}{b}\left(\frac{c_{2,\lim}}{c_k} - a\right) \tag{59}$$

In (59) $c_{2,\lim}$ is defined by expression (2) and a, b are defined by Eq. (58).

8. CONCLUSIONS

The exact solutions of the linear Pochhammer – Chree equation for propagating harmonic axisymmetric longitudinal waves $L(0, m)$ in a cylindrical rod, were analyzed.

Spectral analysis of the matrix dispersion equation for longitudinal axially symmetric modes ($L(0, m)$, $m > 0$) of Pochhammer – Chree waves was done, revealing that no longitudinal modes can propagate at the shear bulk wave phase speed (c_2).

Variation of wave polarization on the free surface due to variation of Poisson's ratio and circular frequency was analyzed. It was found that at positive Poisson's ratios there was phase speed c_k (value of this speed depends upon Poisson's ratio) at which longitudinal component U_z of the fundamental longitudinal mode vanishes, while radial component U_r does not. It is also observed that polarization of the considered Pochhammer – Chree waves for both mild auxetics and non-auxetics exhibits abnormal behavior in the vicinity of the bulk shear wave speed (c_2).

ACKNOWLEDGEMENTS

The authors are thankful to Professor S. Sekerzh-Zenkovich (IPMech, Russia) for the useful discussions.

REFERENCES

1. Pochhammer, L., "Ueber die Fortpflanzungsgeschwindigkeiten Kleiner Schwingungen in Einem Unbegrenzten Isotropen Kreiscylinder," *Journal für die Reine und Angewandte Mathematik*, **81**, pp. 324-336 (1876).
2. Chree, C., "Longitudinal Vibrations of a Circular Bar," *The Quarterly Journal of Pure and Applied Mathematics*, **21**, pp. 287-298 (1886).
3. Chree, C., "The Equations of An Isotropic Elastic Solid in Polar and Cylindrical Coordinates, Their Solutions and Applications," *Transactions of the Cambridge Philosophical Society*, **14**, pp. 250-309 (1889).
4. Field, G. S., "Velocity of Sound in Cylindrical Rods," *Canadian Journal of Research*, **5**, pp. 619-624 (1931).
5. Field, G. S., "Longitudinal Waves in Cylinders of Liquid, in Hollow Tubes and in Solid Rods," *Canadian Journal of Research,* **11**, pp. 254-263 (1934).
6. Field, G. S., "Dispersion of Supersonic Waves in Cylindrical Rods," *Physical Review*, **57**, 1188 (1940).
7. Shear, S. K. and Focke, A. B., "The Dispersion of Supersonic Waves in Cylindrical Rods of Polycrystalline Silver, Nickel, and Magnesium," *Physical Review*, **57**, pp. 532-537 (1940).
8. Bancroft, D., "The Velocity of Longitudinal Waves in Cylindrical Bars," *Physical Review*, **59**, pp. 588-593

https://doi.org/10.1017/jmech.2018.13 Published online by Cambridge University Press

(1941).

9. Hudson, G. E., "Dispersion of Elastic Waves in Solid Circular Cylinders," *Physical Review*, **63**, pp. 46-51 (1943).
10. Holden, A. H., "Longitudinal Modes of Elastic Waves in Isotropic Cylinders and Slabs," *The Bell System Technical Journal*, **30**, pp. 956-969 (1951).
11. Adem, J., "On the Axially-Symmetric Steady Wave Propagation in Elastic Circular Rods," *Quarterly of Applied Mathematics*, **12**, pp. 261-275 (1954).
12. Redwood, M. and Lamb, J., "On Propagation of High Frequency Compressional Waves in Isotropic Cylinders," *Proceedings of the Physical Society of London*, **70**, pp. 136-143 (1957).
13. Mindlin, R. D. and McNiven, H. D., "Axially Symmetric Waves in Elastic Rods," *Transactions of ASME, Journal of Applied Mechanics*, **27**, pp. 145-151 (1960).
14. McNiven, H. D. and Perry, D. C., "Axially Symmetric Waves in Infinite, Elastic Rods," *Journal of the Acoustical Society of America*, **34**, pp. 433-437 (1962).
15. Onoe, M., McNiven, H. D. and Mindlin, R. D., "Dispersion of Axially Symmetric Waves in Elastic Rods," *Transactions of ASME, Journal of Applied Mechanics,* **29**, pp. 729-734 (1962).
16. Meeker, T. R. and Meitzler, A. H., "Guided Wave Propagation in Elongated Cylinders and Plates," In, *Physical Acoustics, Principles and Methods*, Academic Press, N.Y., **1A**, pp. 111-167 (1964).
17. Kolsky, H., "Stress Waves in Solids," *Journal of Sound and Vibration,* **1**, pp. 88-110 (1964).
18. Hutchinson, J. R. and Percival, C. M., "Higher Modes of Longitudinal Wave Propagation in Thin Rod," *Journal of the Acoustical Society of America*, **44**, pp. 1204-1210 (1968).
19. Zemanek, J., "An Experimental and Theoretical Investigation of Elastic Wave Propagation in a Cylinder," *Journal of the Acoustical Society of America,* **51**, pp. 265-283 (1972).
20. Thurston, R. N., "Elastic Waves in Rods and Clad Rods," *Journal of the Acoustical Society of America,* **64**, pp. 1-37 (1978).
21. Pao, Y.-H. and Mindlin, R. D., "Dispersion of Flexural Waves in An Elastic, Circular Cylinder," *Transactions of ASME, Journal of Applied Mechanics,* **27**, pp. 513-520 (1960).
22. Valsamos, G., Casadei, F. and Solomos, G., "A Numerical Study of Wave Dispersion Curves in Cylindrical Rods with Circular Cross-Section," *Applied and Computational Mechanics*, **7**, pp. 99-114 (2013).
23. Kuznetsov, S. V., "Lamb Waves in Anisotropic plates (Review)," *Acoustical Physics*, **60**, pp. 95-103 (2014).
24. Kuznetsov, S. V., "Love Waves in Nondestructive Diagnostics of Layered Composites. Survey," *Acoustical Physics*, **56**, pp. 877-892 (2010).
25. Tyutekin, V. V. and Boiko, A. I., "Helical Normal Waves Near a Cylindrical Cavity in An Elastic Medium," *Acoustical Physics*, **56**, pp. 141-144 (2010).
26. Pavić, G., Chevillotte, F. and Heraud J., "Dynamics of Large-Diameter Water Pipes in Hydroelectric Power Plants," *Journal of Physics, Conference Series*, **813**, pp. 1-5 (2017).
27. Sharma, G. S., Skvortsov, A., MacGillivray, I. and Kessissoglou, N., "Acoustic Performance of Gratings of Cylindrical Voids in a Soft Elastic Medium with a Steel Backing," *Journal of the Acoustical Society of America*, **141**, pp. 4694-4704 (2017).
28. Altman, W. and De Oliveira, A. M., "Physical Components of Tensors," *CRC Press*, 2014. ISBN: 9781482263824.

(Manuscript received November 3, 2017,
accepted for publication February 21, 2018.)

https://doi.org/10.1017/jmech.2018.13 Published online by Cambridge University Press